Supporting Information for

Adjustable comb/bottlebrush fast UV-curable epoxy-based form-stable phase change materials with high encapsulation rate and ultralow enthalpy loss

Yu Fan[a], Yanyun Li[a], Xinyuan Tang[a], Junying Zhang[a], Jue Cheng[a]*, Qingsong Lian[b]*

[a]Key Laboratory of Carbon Fiber and Functional Polymers, Ministry of Education, Beijing University of Chemical Technology, Beijing 100029, China

[b]College of Materials Science and Engineering, North University of China, Taiyuan 030051, China

* Corresponding author and E-mail address:

chengjue@mail.buct.edu.cn (Jue Cheng),

lianqs@nuc.edu.cn (Qingsong Lian),

Tel. /fax: +86 10 64425439

Table of Contents

Abbreviations list

PCMs	phase change materials	**TES**	thermal energy storage
FSPCMs	Form-stable PCMs	**SLPCMs**	solid-liquid PCMs
PEG	polyethylene glycol	**PU**	polyurethane
PE	polyethylene	**EP**	epoxy resin
ODT	1-Octadecanethiol	**CNT**	carbon nanotubes
HDT	1,6-Hexanedithiol	**ODA**	octadecylamine
FM	furfuryl mercaptan	**BMI**	bismaleimide
FT-IR	Fourier transform infrared	**TGA**	thermogravimetric analysis
XRD	X-ray diffraction	**POM**	optical microscopy
DSC	differential scanning calorimetry	**SEM**	scanning electron microscope
DMA	dynamic mechanical analyses	**UV**	ultra-violet
Tm	melting temperature	ΔH_f	latent heat during freezing

Tg	glass transition temperature	ΔH_m	latent heat during melting
D-A	Diels-Alder	ΔG	free energy of mixing

1. The main chemical structures in this study

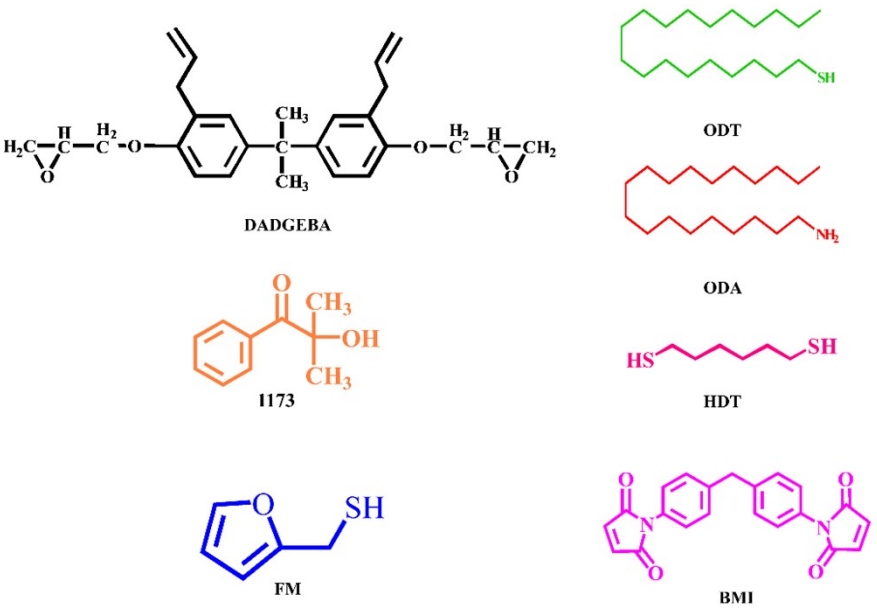

Scheme. S1 The structures of DADGEBA, ODT, ODA, 1173, HDT, FM, and BMI

2. Characterization of xD18

2.1 The chemical equation of xD18

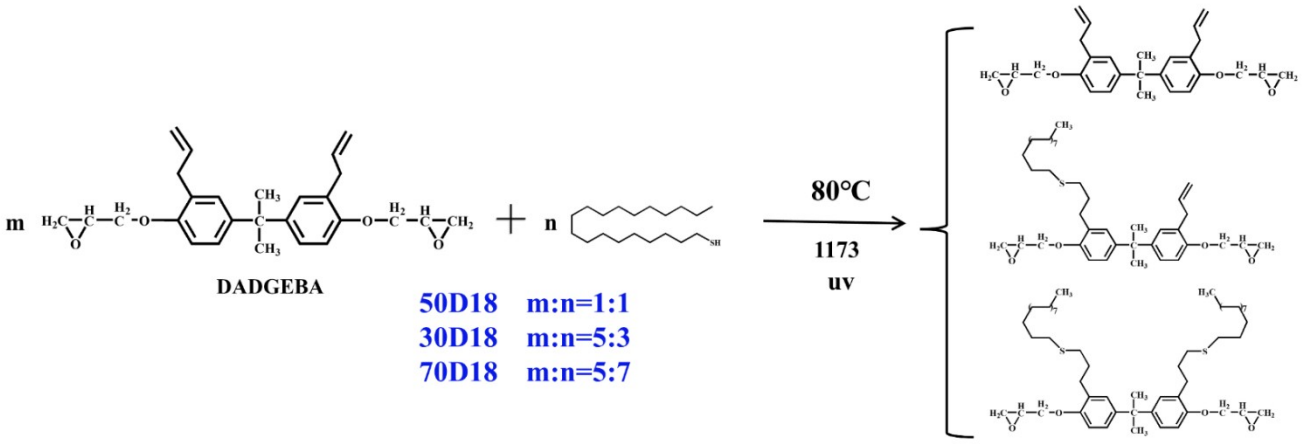

Scheme S2 Thiol-ene click chemistry of DADGEBA and ODT

2.2 ^{1}H-NMR spectra

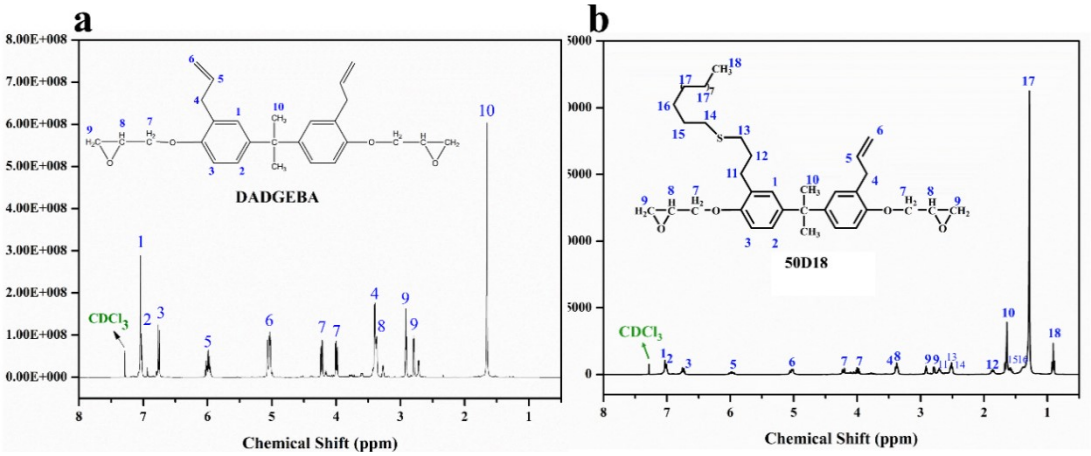

Fig. S1 ^{1}H-NMR spectra of (a) DADGEBA; and (b) 50D18 samples

^{1}H-NMR spectra shown in **Fig. S1** further proved the consumption of double bonds, because the chemical shifts of the unsaturated H atoms corresponding to allyl groups in DADGEBA (at 3.37, 5.95, and 5.00 ppm) disappeared and moves to 2.69, 2.49, and 1.84 ppm (attributed to D18).

2.3 FTIR spectra of the xD18

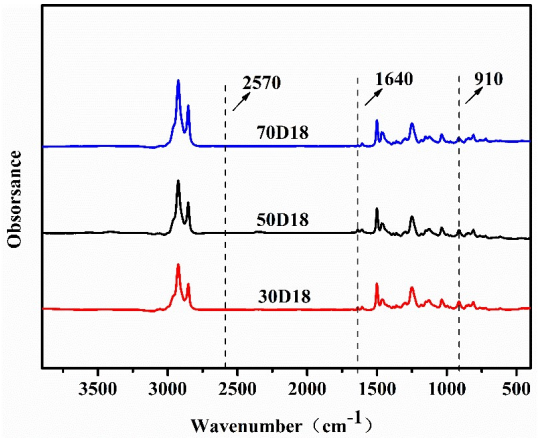

Fig. S2 FTIR spectrum of xD18 samples

2.4 DSC analysis of the xD18

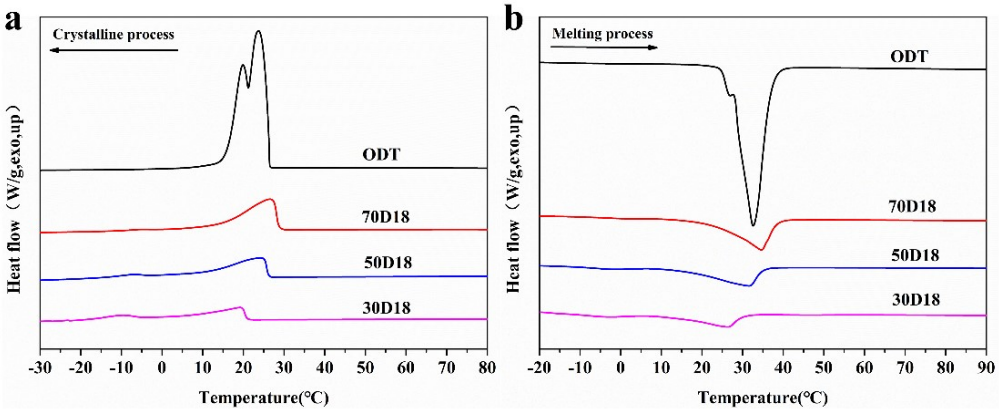

Fig. S3 DSC curves of xD18 and ODT samples

3. Characterization of the un-50DA18-y and 50DA18-y

3.1 FTIR spectra

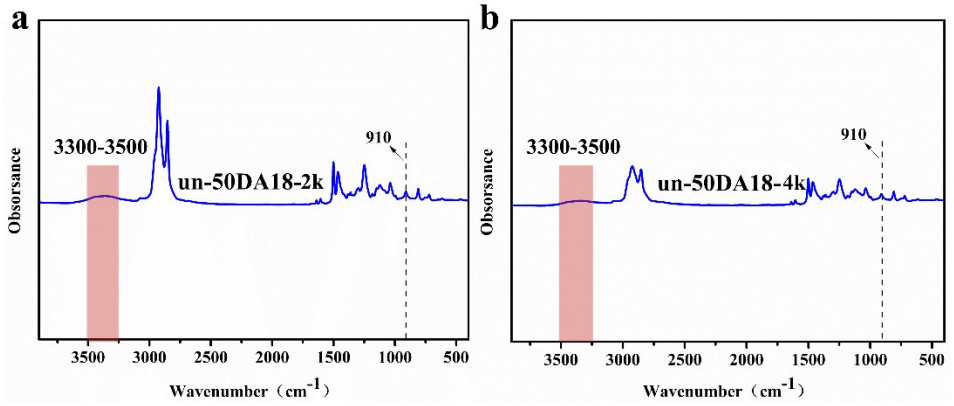

Fig. S4 FTIR spectrum of (a) un-50DA18-2k sample; and (b) un-50DA18-4k sample

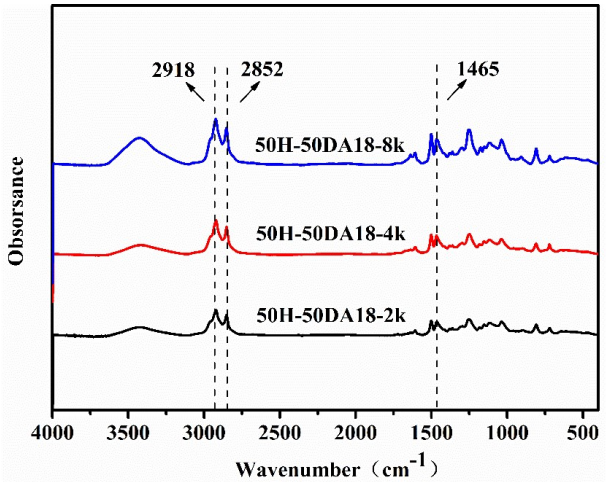

Fig. S5 FTIR spectra of the 50H-50DA18-2k, 50H-50DA18-4k, and 50H-50DA18-8k samples

3.2 DSC analysis

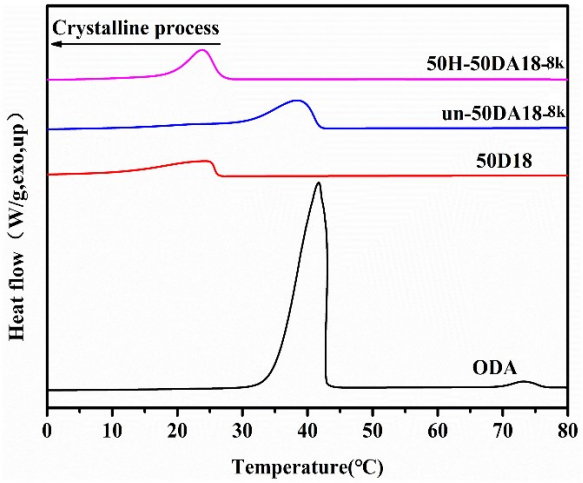

Fig. S6 Crystalline process of ODA, 50D18, un-50DA18-8k systems, and 50H-50DA18-8k systems.

Table S1 Thermal characteristics of un-xDA18 and 30H-xDA18

Sample	T_m (°C)	ΔH_m (Jg^{-1})	ΔH^T_m (Jg^{-1})	ΔH_mloss	T_f (°C)	ΔH_f (Jg^{-1})	ΔH^T_f (Jg^{-1})	ΔH_floss
un-30DA18	40.5	54.7	121.1	54.8%	26.1	48.2	120.8	60.0%
un-50DA18	46.5	74.6	131.9	43.4%	33.8	61.6	129.7	52.5%
un-70DA18	51.1	86.5	140.4	38.4%	39.5	72.9	140.0	47.9%
30H-30DA18	34.5	35.4	51.9	31.8%	16.3	34.9	45.7	23.6%
30H-50DA18	42.4	45.9	71.1	35.4%	21.6	41.4	58.7	29.5%
30H-70DA18	44.3	52.5	82.6	36.4%	28.1	48.0	69.6	31.0%

Notes: Tm, Tf, ΔHm, and ΔHf can be obtained directly from DSC curves; ΔHm^T and ΔHf^T of the un-xDA18 samples were calculated by summing the melting or freezing enthalpies of the xDA18, ODT, and ODA parts (respectively multiplying the weight percentage of xDA18, ODT, and ODA with the melting or freezing enthalpies of the xDA18, ODT, and ODA); ΔHm^T and ΔHf^T of the 30H-xDA18 samples were calculated by multiplying the weight percentage of un-xDA18 with the melting or freezing enthalpies of the un-xDA18 samples; ΔHm loss (%) of the 30H-xDA18 samples was the percentage of the difference between ΔHm (ΔHf) and ΔHm^T (ΔHf^T)

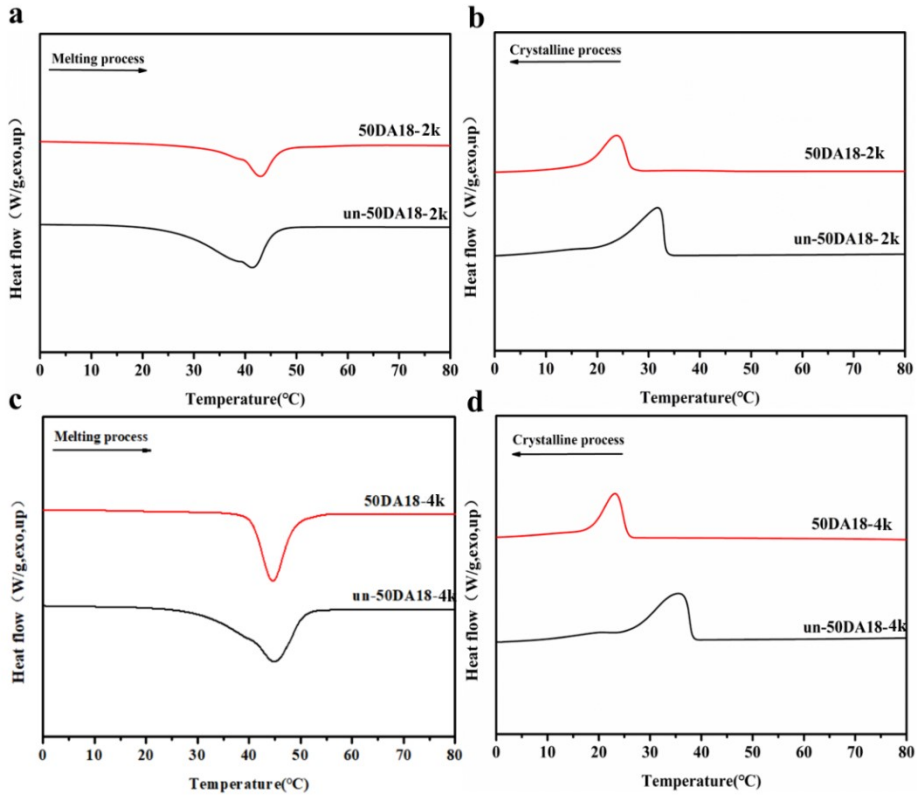

Fig. S7 DSC curves of (a) and (b) un-50DA18-2k and 50H-50DA18-2k samples; (c) and (d) un-50DA18-4k and 50H-50DA18-4k samples.

4. Characterization of the 50H-50DA18$_{Pa-m}$-y

4.1 Leakage test

Table S2 Mass change of all samples after phase change

Sample	Original (gram)	After heating (gram)	Leakage problem
50H-50DA18-2k	1.613	1.613	No
50H-50DA18$_{Pa-30}$-2k	1.423	1.423	No
50H-50DA18$_{Pa-40}$-2k	1.466	1.466	No
50H-50DA18$_{Pa-50}$-2k	1.334	1.334	No
50H-50DA18$_{Pa-60}$-2k	1.551	1.427	8%
50H-50DA18$_{Pa-70}$-2k	1.554	1.290	17%
50H-50DA18-4k	1.731	1.731	No
50H-50DA18$_{Pa-30}$-4k	1.501	1.500	No
50H-50DA18$_{Pa-40}$-4k	1.332	1.332	No
50H-50DA18$_{Pa-50}$-4k	1.621	1.621	No
50H-50DA18$_{Pa-60}$-4k	1.550	1.504	3%
50H-50DA18$_{Pa-70}$-4k	1.713	1.559	9%
50H-50DA18-8k	1.433	1.433	No
50H-50DA18$_{Pa-30}$-8k	1.612	1.612	No
50H-50DA18$_{Pa-40}$-8k	1.555	1.555	No
50H-50DA18$_{Pa-50}$-8k	1.675	1.675	No
50H-50DA18$_{Pa-60}$-8k	1.435	1.435	No
50H-50DA18$_{Pa-70}$-8k	1.774	1.703	4%

4.2 DSC analysis

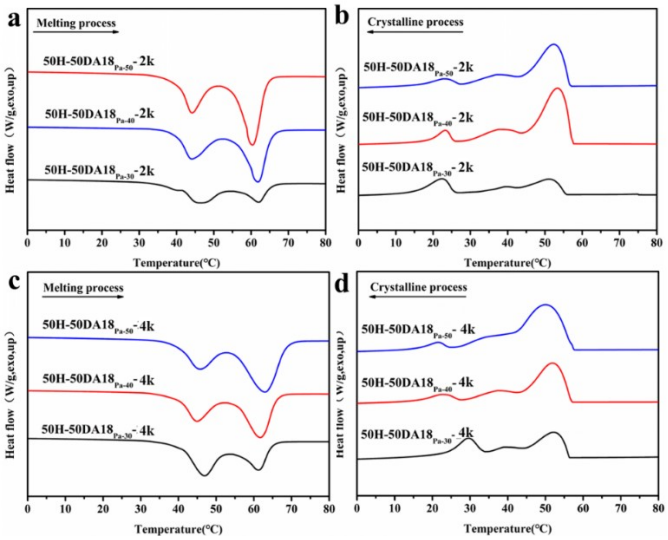

Fig. S8 DSC curve of 50H-50DA18A$_{Pa-m}$-2k and 50H-50DA18A$_{Pa-m}$-4k samples.

5. Characterization of the 30H-xDA18 and 30H-xDA18$_{Pa-m}$

5.1 DSC analysis

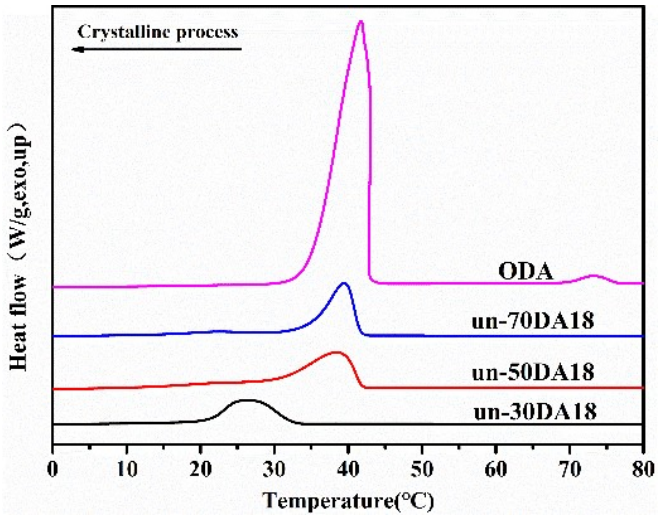

Fig. S9 The freezing process of DSC curves for ODA and un-xDA18 samples

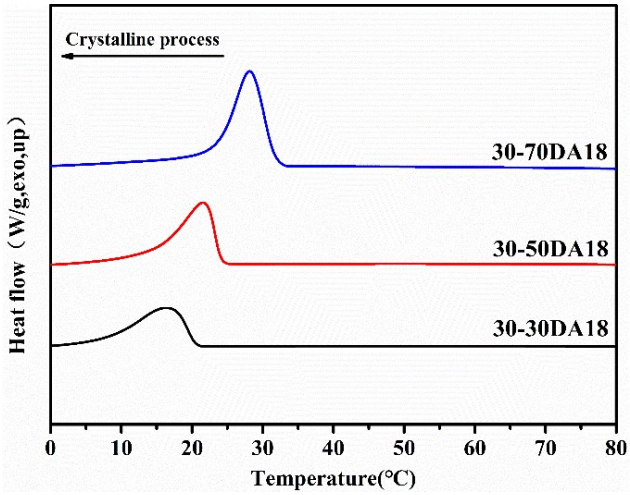

Fig. S10 The freezing process of DSC curves for 30H-xDA18 samples

Table S3 Thermal characteristics of 30H-xDA18$_{Pa-m}$ systems

Sample	ΔH_m (Jg^{-1})	ΔH^T_m (Jg^{-1})	ΔH_m loss	ΔH_f (Jg^{-1})	ΔH^T_f (Jg^{-1})	ΔH_f loss
30H-30DA18$_{Pa-30}$	88.0	91.9	4.2%	86.7	91.0	4.7%
30H-50DA18$_{Pa-30}$	93.7	98.1	4.5%	89.5	94.9	5.7%
30H-70DA18$_{Pa-30}$	98.9	103.9	4.8%	93.5	100.2	6.7%
30H-30DA18$_{Pa-40}$	109.1	110.7	1.4%	107.9	109.7	1.6%
30H-50DA18$_{Pa-40}$	113.9	116.1	1.9%	110.5	113	2.2%

Notes: ΔHm^T and ΔHf^T of the 30H-xDA18$_{Pa-m}$ systems were calculated by summing the melting or freezing enthalpies of the 30H-xDA18$_{Pa-0}$ parts (multiplying the weight percentage of 30H-xDA18$_{Pa-0}$ with the melting or freezing enthalpies of the 30H-xDA18$_{Pa-0}$ samples) and the paraffin parts (multiplying the weight percentage of paraffin with the melting or freezing

enthalpies of paraffin).; ΔHm loss (%) of the 30H-xDA18 $_{Pa\text{-}m}$ samples was the percentage of the difference between ΔHm (ΔHf) and ΔHm^T (ΔHf^T).

5.2 Leakage test

Table S4 Mass change of all samples after phase change

Sample	Original (gram)	After heating (gram)	Leakage problem
30H-30DA18	1.309	1.309	No
30H-30DA18$_{Pa\text{-}30}$	1.412	1.412	No
30H-30DA18$_{Pa\text{-}40}$	1.443	1.443.6	No
30H-30DA18$_{Pa\text{-}50}$	1.533	1.456	5%
30H-50DA18	1.512	1.512	No
30H-50DA18$_{Pa\text{-}30}$	1.551	1.551	No
30H-50DA18$_{Pa\text{-}40}$	1.594	1.594	No
30H-30DA18$_{Pa\text{-}50}$	1.796	1.509	16%
30H-70DA18	1.631	1.631	No
30H-70DA18$_{Pa\text{-}30}$	1.501	1.501	No
30H-70DA18$_{Pa\text{-}30}$	1.650	1.551	6%

6. Photothermal conversion of the FSPCMs

The solar-thermal energy storage efficiency (η) of the PCMs under the light irradiation was estimated by the ratio between the stored thermal energy and the received light energy using the following equation:[1]

$$\eta = \frac{Q_s}{Q} = \frac{m \times \Delta H}{P \times A \times t}$$

where Qs is the stored thermal energy by the PCMs, Q is the received light energy by the sample, m (~2.6 g) is the mass of the nanocomposite sample, P (1500 W m^{-2}) is the intensity of the simulated solar light, A (6.76 cm^2) is the surface area of the nanocomposite exposed to light, t (500s) is the duration of light irradiation for heating the composite from a lower temperature (T1) to a higher temperature (T2), and ΔH is the enthalpy change of the composite between the temperature range (T1 to T2) and can be obtained by the DSC measurements. When the temperature of the PCMs increased from 30 °C to 70 °C, which corresponded to an enthalpy change (ΔH) of 136.6 J g^{-1}, a storage efficiency (η) is calculated to be 70% for this period.

7. Characterization of the 50DF18 sample

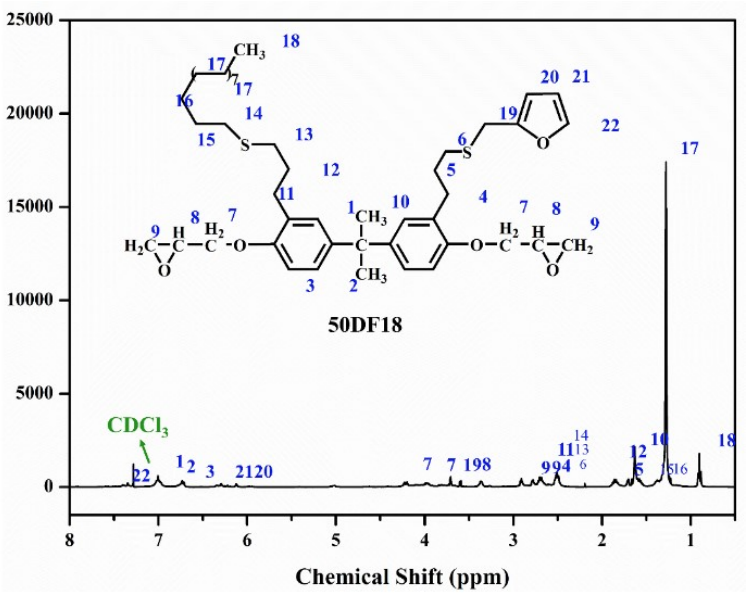

Fig. S11 NMR of the 50DFA18 sample

Table S5 Thermal characteristics of the 50DF18, un-50DFA18 and 50DFA18 samples

Sample	T_m (°C)	ΔH_m (Jg^{-1})	ΔH^T_m (Jg^{-1})	ΔH_mloss (%)	T_f (°C)	ΔH_f (Jg^{-1})	ΔH^T_f (Jg^{-1})	ΔH_mloss (%)
50DF18	32.5	53.7	59.8	10.2	26.3	53.5	57.4	7.0
un-50DFA18	46.0	70.4	88.6	20.5	36.4	56.9	88.4	35.6
50DFA18	34.4	20.4	59.5	65.7	14.1	19.8	48.1	58.8

Notes: Tm, Tf, ΔHm, and ΔHf can be obtained directly from DSC curves; ΔHm^T and ΔHf^T of the 50DF18 sample was calculated by multiplying the weight percentage of 50D18 with the melting or freezing enthalpies of the 50D18 samples. ΔHm^T and ΔHf^T of the un-50DFA18 sample was calculated by summing the melting or freezing enthalpies of the 50DF18 and ODA parts (respectively multiplying the weight percentage of 50DF18 and ODA with the melting or freezing enthalpies of the 50DF18 and ODA); ΔHm^T and ΔHf^T of the 50DFA18 sample was calculated by multiplying the weight percentage of un-50DFA18 with the melting or freezing enthalpies of theun-50DFA18 samples. △Hm loss (%) of the 50DF18, un-50DFA18 and 50DFA18 samples was the percentage of the difference between ΔHm (ΔHf) and ΔHm^T (ΔHf^T).

8. Thermal characteristics of the other samples

Table S6 Thermal characteristics of the other samples

system	T_m (°C)	ΔH_m (Jg^{-1})	ΔH^T_m (Jg^{-1})	ΔH_m loss (%)	T_f (°C)	ΔH_f (Jg^{-1})	ΔH^T_f (Jg^{-1})	ΔH_m loss (%)
ODT	32.7	236.9	/	/	23.3	228.8	/	/
ODA	54.14	306.6	/	/	41.75	306.2	/	/
Paffin	60.93	223.7	/	/	55.26	221.9	/	/
30D18	26.2	46.9	69.1	32.1	19.1	46.7	66.8	30.1
50D18	31.5	69.2	96.5	28.3	22.8	66.4	93.2	28.8
70D18	34.6	83.8	116	27.9	26.5	83.2	112.1	25.8

Notes: Tm, Tf, ΔHm, and ΔHf can be obtained directly from DSC curves; ΔHm^T and ΔHf^T of the xD18 samples were calculated by multiplying the weight percentage of ODT with the melting or freezing enthalpies of the ODT samples. △Hm loss (%) of the xD18 samples was the percentage of the difference between ΔHm (ΔHf) and ΔHm^T (ΔHf^T).

Reference

1 L. Zhang, R. Li, B. Tang and P. Wang, *Nanoscale*, 2016, **8**, 14600-14607.